7 Particle Physics at DESY/HERA (H1)

Katharina Müller, K. Nowak, P. Robmann, C. Schmitz, A. Schöning, U. Straumann, and P. Truöl

in collaboration with: N. Berger, M. Del Degan, C. Grab, G. Leibenguth, M. Sauter and T. Zimmermann, Institut für Teilchenphysik der ETH, Zürich; S. Egli, R. Eichler, M. Hildebrandt, and R. Horisberger, Paul Scherrer Institut, Villigen, and 37 institutes outside Switzerland

(H1 - Collaboration)

7.1 Summary

Two data taking periods with the proton energy reduced from its nominal value of 920 GeV between March 21, 2007 and June 30, 2007 ended the experimental phase of the H1-collaboration at the HERA electron-proton storage ring. Since then the detector has been dismantled and the collaboration concentrates on the analysis of the different data sets from the post-upgrade HERA-II phase (2004-2007, $\mathcal{L}$ =238 pb^{-1} e^-, $\mathcal{L}$ =219 pb^{-1} e^+) and the pre-upgrade HERA-I phase (1993-2000, $\mathcal{L}$ =118 pb^{-1} $e^\pm$). Figure 7.1 shows how the integrated luminosity was accumulated over the years. During the low energy run 6.2 pb^{-1} and 12.4 pb^{-1} were collected with 27.4 GeV positrons colliding with 575 or 460 GeV protons, respectively.

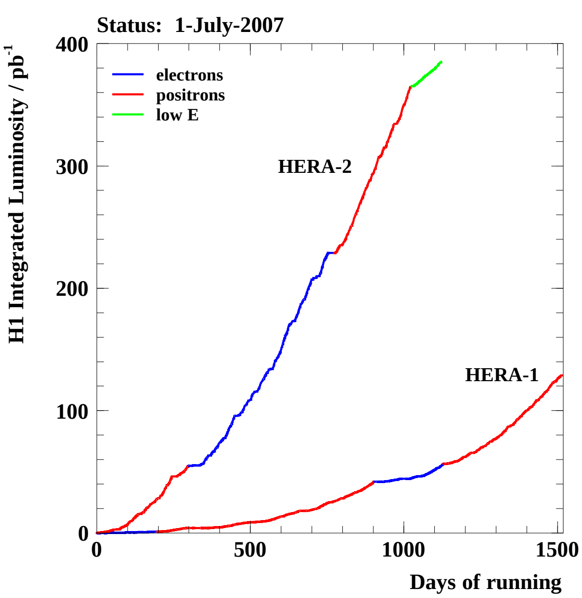

Figure 7.1:
Integrated luminosity as a function of running time 1993-2000 (HERA-I), and 2004-2007 (HERA-II).

Eleven publications ((1)-(11)) and a fair number of contributions to the summer 2007 high-energy physics conference EPS2007 in Manchester ((12),(13)-(31)) attest to the continuing effort of the collaboration exploring proton structure and testing quantum chromodynamics (QCD) predictions. This program entails the precise determination of the neutral and charged electroweak current cross sections at high momentum transfer leading to parton density functions (PDF) in pre-HERA inaccessible domains of Bjorken x and momentum transfer Q^2, precise measurements of the running coupling constant α_s, diffractively produced final states, hidden and open charm and beauty production as well as searches for states outside the Standard Model.

Our analysis effort concentrated on events with isolated photons produced in either photoproduction ($Q^2 \approx 0$), as discussed below (Sec. 7.3), or deep inelastic scattering ($Q^2 > 4$ GeV^2) as described in the thesis of Carsten Schmitz (32), the publication which resulted from it (9) or in previous annual reports (33) in some detail. The technical paper dealing with our hardware contribution to the upgraded H1-detector, the five-layer inner multiwire proportional chamber (CIP2000) and the z-vertex trigger derived from it, has appeared too (34).

New results, partly preliminary (35), which deserve to be mentioned, concern the following topics:

- direct measurement of the longitudinal structure function F_L at medium Q^2; combined PDF-fit of ZEUS and H1 data (HERA I);
- multi-jets at high and low Q^2 leading to an improved determination of α_s;
- photo-produced diffractive dijets, diffractive ρ- and ϕ-mesons, inelastic J/ψ- and D^*-mesons, and prompt photons;
- searches for leptoquarks, lepton flavor violation, excited neutrinos, and exotic baryons (charmed pentaquark);
- strangeness and D^*-meson production in deep inelastic scattering, and charm fragmentation.

7.2 Structure functions

The primary goal of the low energy runs was the determination of the longitudinal structure function F_L appearing in the inclusive deep inelastic cross section as (see also last years annual report (33)):

$$\frac{d^2\sigma}{dxdQ^2} = \frac{2\pi\alpha^2 Y_+}{Q^4 x}\left[F_2(x,Q^2) - f(y)\cdot F_L(x,Q^2)\right] ,$$

with $y \equiv Q^2/sx$, $Y_+ \equiv 1 + (1-y)^2$ and $f(y) \equiv y^2/Y_+$. It is possible to extract F_L directly from two or more cross section measurements at fixed Bjorken x and negative momentum transfer squared Q^2 by varying the fractional electron energy loss y, which is possible by changing the centre-of-mass energy $\sqrt{s} = \sqrt{4E_eE_p}$ via the proton beam energy. F_L is then determined from a Rosenbluth plot of $F_2(x,Q^2)$ versus y^2/Y_+ using the different values of s available. This procedure has been successfully applied already,

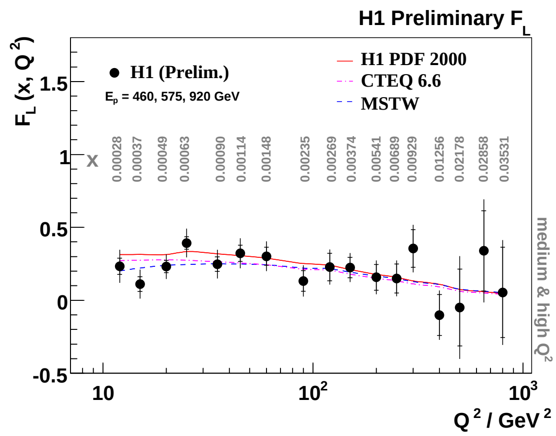

Figure 7.2: Longitudinal structure function as function of Q^2. The value of x for each data point is indicated [35].

as shown in Fig. 7.2, to the medium Q^2 2007 data. The new data confirm the behavior predicted by the PDF-analysis of HERA-I data. The latter have now been incorporated in a combined analysis of the data from both HERA-collaborations, results of which are shown in Figs. 7.3 and 7.4. A consistent treatment of the systematic uncertainties of both data sets,

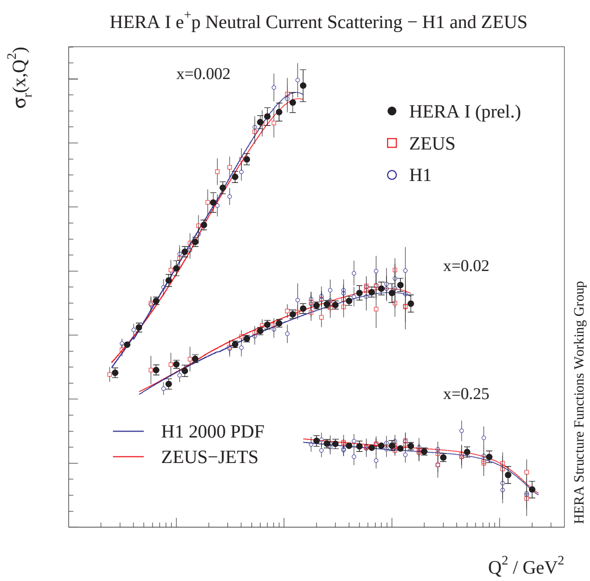

Figure 7.3: Examples of HERA-I data sets from the ZEUS- and the H1-collaborations entering the common PDF-fit.

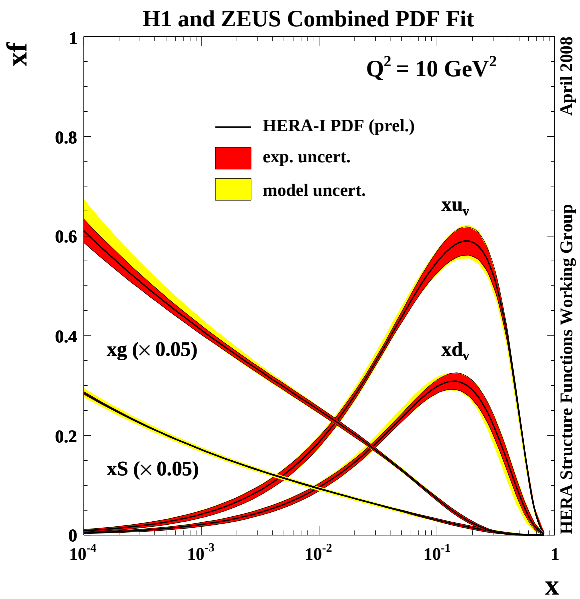

Figure 7.4:
A typical result at Q^2=10 GeV^2 indicates a better constrained gluon distribution at high and low x.

choice of parametrisation at the momentum transfer Q_0^2, where the DGLAP-evolution of the PDF's is started, incorporation of correlations and a suitable exploits the full potential for precision of the HERA-data. At present the consequences are most visible for the gluon density at low x. Clearly it is planned to continue with this work, once the even higher statistics HERA-II data have been analyzed completely, particularly in view of the need for accurate PDF's for theoretical predictions at the Large Hadron Collider (LHC).

7.3 Isolated photons in photoproduction and deep inelastic scattering

In the past years our analysis group, lead by Dr. Katharina Müller, focused on the analysis of events with isolated photons. The analyses profit a lot from a close collaboration with the local theory group of Thomas Gehrmann.

Isolated photons with high transverse momentum in the final state are a direct probe of the dynamics of the hard scattering process, since they are directly observable without large corrections due to hadronisation and fragmentation. A good understanding of the standard model production mechanism of isolated photons is important for the understanding of the background to a light Higgs decaying into two photons at LHC as well as for searches for physics beyond the standard model.

Common to all analyses is the identification of the photon as an isolated electromagnetic cluster with no track pointing to it in order to reject charged particles. To ensure isolation of the photon, the fraction z of the transverse energy of the photon-jet (jet containing the photon) carried by the photon candidate has to be larger than 90%. The experimental difficulty is the separation of the photons from the decay products of neutral mesons, mainly π^0 or η, since at high energies the decay photons are not resolved but reconstructed in one single electromagnetic cluster. The photon signal is extracted by a shower shape analysis which uses six discriminating shower shape functions in a likelihood analysis.

In the thesis of Carsten Schmitz on isolated photons in deep inelastic scattering (9; 32) it has been shown that the leading order (LO) calculation (36) significantly underestimates the cross section of the production of isolated photons by roughly a factor two, in particular at low Q^2. A next to leading order calculation (37) which is only available for the exclusive process with a photon and a hadronic jet in the final state is higher than the LO prediction and describes the data well in shape but is also too low in absolute normalisation.

In the past months the analysis has been extended to the analysis of less isolated photons which gives access to the quark-to-photon fragmentation function (38). The latter cannot be calculated in perturbative QCD but

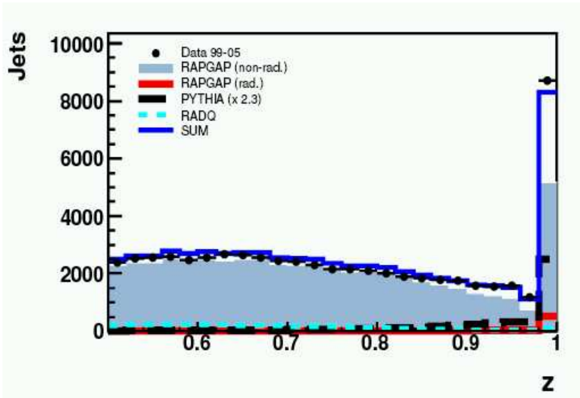

Figure 7.5: Distribution of the isolation parameter $z \equiv E_T^\gamma / E_T^{photonjet}$. The shaded area corresponds to the background contribution.

has to be determined by the experiments, which was only done by the ALEPH collaboration (39). The cross section is measured in bins of z, where z is the isolation parameter defined above.

Figure 7.5 shows the measured z distribution. The shaded area corresponds to the background and the white area can be attributed to the photon contribution. Whereas in the isolated case ($z > 0.9$) a clear signal of the photon is visible the background is dominating by far for photons close to a hadronic environment ($z < 0.9$). The extraction of less isolated photons therefore mainly requires a detailed understanding of the shower shapes of the background. Preliminary results are expected to be ready this summer.

In photoproduction (PhD thesis of Krzysztof Nowak) at very low Q^2 the scattered electron escapes detection through the beam pipe. The exchanged quasi-real photon either interacts directly with a parton from the proton (direct contribution) or resolves into partons which take part in the interaction (resolved contribution). Hence, the cross section yields information on the quark and gluon densities in the photon and the proton with different and generally lower corrections for hadronisation than in jet measurements. The analysis extends the phase space of the previous

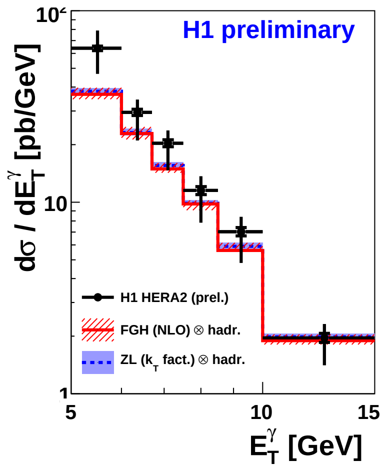

Figure 7.6: Inclusive prompt photon single differential cross sections as function of E_T^γ. The measured cross section is compared to two calculations.

H1 measurement in photoproduction (40) towards larger pseudorapidities of the photon and lower event inelasticities. The data used for the measurement were collected during the years 2004-2007 corresponding to a total integrated luminosity of 340 pb^{-1}, increased by a factor of three over the previous measurement. Following the results of the Bachelor thesis of Arno Gadola who analysed the separation of photons and π^0 at high transverse energies, the analysis is further extended to transverse energies up to 15 GeV. Preliminary results will be shown this spring. Figure 7.6 shows the single differential inclusive cross section as a function of transverse energy of the photon. The data are compared to a NLO calculation (41), denoted by FGH), and a calculation based on the k_T factorisation approach which uses the unintegrated quark and gluon densities of the proton and the photon according to the Kimber-Martin-Ryskin prescription (42) (ZL). Both calculations are slightly lower than the data most significantly at low E_T^γ. The momentum fraction of the partons in the photon (x_γ) and in the proton (x_p) can be determined in the exclusive sample with an isolated photon and an additional hadronic jet

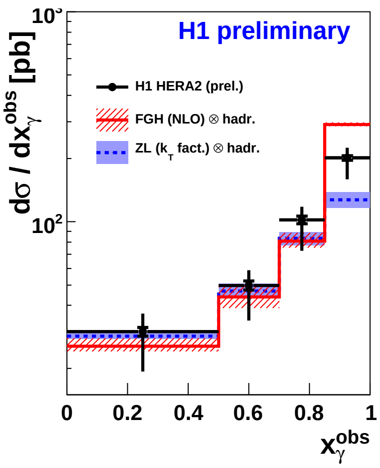

Figure 7.7: Exclusive (photon plus jet) cross sections as a function of x_γ. The measured cross section is compared to two calculations.

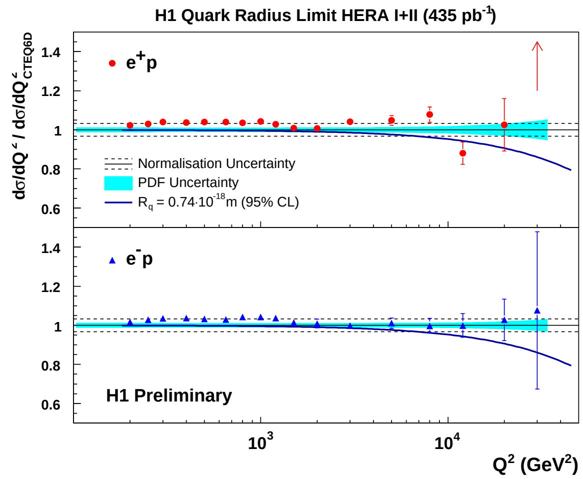

Figure 7.8: The good agreement with the behavior expected for the neutral current e^+p cross section at high Q^2 sets an upper limit on the quark radius of 0.74 attometer [35].

from the kinematics of the photon and the jet. The cross section as a function of x_γ is shown in Fig. 7.7. The distributions are described reasonably well by the two calculations.

7.4 Other results from recent analyses

The ultimate spatial resolution of the HERA *electron microscope* is demonstrated by the high Q^2 neutral current cross section shown in Fig. 7.8, which exhibits the deviations expected if quarks were extended objects.

That a measurement of the relative jet rates at different Q^2, for which some experimental errors cancel, is sensitive to the strong coupling α_s has been shown by H1 previously. These analyses have now been extended to lower Q^2 than before and at higher Q^2 to include both HERA-I and HERA-II data. Figs. 7.9 and 7.10 show the results for the running coupling.

The analysis yields for low Q^2:

$$\alpha_s(M_Z) = 0.1186 \pm 0.0014^{+0.0132}_{-0.0101} \pm 0.0021$$

and for high Q^2:

$$\alpha_s(M_Z) = 0.1182 \pm 0.0008^{+0.0041}_{-0.0031} \pm 0.0018 \quad ,$$

where the first error given is experimental, the second comes from the model (scale) dependence and the last is introduced by the uncertainty of PDF's. Comparison with results from ZEUS and the world average largely given by e^+e^- collider data shows good agreement.

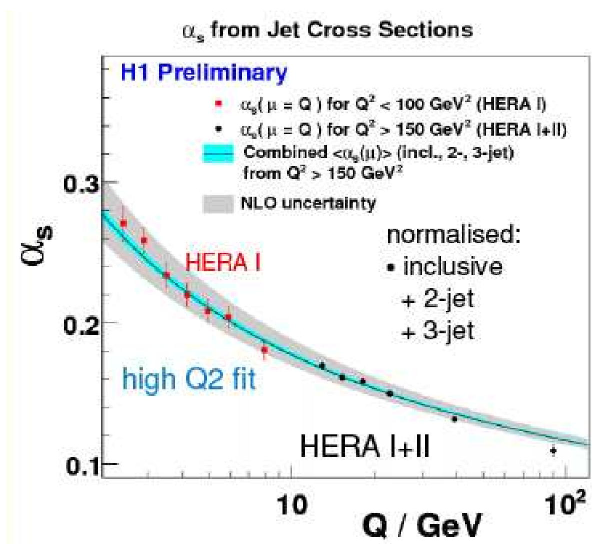

Figure 7.9: Fitted values of $\alpha_s(Q)$ from inclusive jet rates.

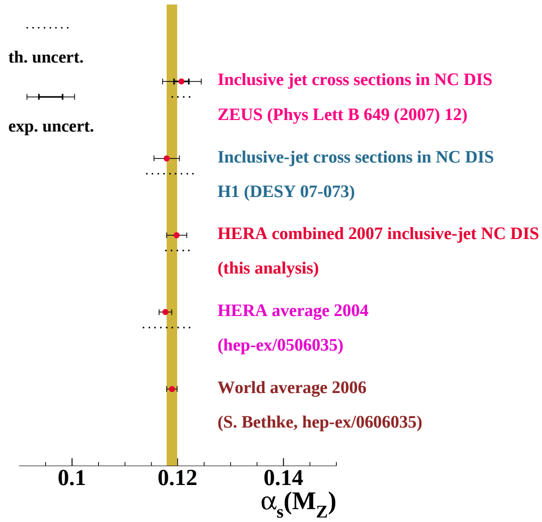

Figure 7.10: Comparison of the HERA results for $\alpha_s(M_Z)$ with the world average.

[1] **Inclusive D^* Meson and Associated Dijet Production in Deep Inelastic Scattering at HERA**, A. Aktas et al. [H1-Coll.], DESY 06 – 240, hep-ex/0701023, Eur.Phys.J. **C51** (2007), 271.

[2] **Search for Lepton Flavour Violation in ep Collisions** A. Aktas et al. [H1-Coll.], DESY 07 – 007, hep-ex/0703004, Eur.Phys.J. **C52** (2007), 833.

[3] **Tests of Factorisation in the Diffractive Production of Dijets in Deep Inelastic Scattering and Photoproduction at HERA**, A. Aktas et al. [H1-Coll.], DESY 07 – 018, hep-ex/0703022, Eur.Phys.J. **C51** (2007), 549.

[4] **Search for Baryonic Resonances Decaying to $\Xi\pi$ in Deep Inelastic Scattering at HERA**, A. Aktas et al. [H1-Coll.], DESY 07 – 045, arXiv:0704.3594 [hep-ex], Eur.Phys.J. **C52** (2007), 507.

[5] **Charged Particle Production in High Q^2 Deep Inelastic Scattering at HERA**, F.D. Aaron et al. [H1-Coll.], DESY 07 – 065, arXiv:0706.2456 [hep-ex], Phys.Lett. **B654** (2007), 148.

[6] **Measurement of Inclusive Jet Production in Deep-Inelastic Scattering at High Q^2 and Determination of the Strong Coupling**, A. Aktas et al. [H1-Coll.], DESY 07 – 073, arXiv:0706:3722 [hep-ex], Phys.Lett. **B653** (2007), 134.

[7] **Dijet Cross Sections and Parton Densities in Diffractive DIS at HERA**, A. Aktas et al. [H1-Coll.], DESY 07 – 115, arXiv:0708.3217 [hep-ex], JHEP **10** (2007), 042

[8] **Measurement of Deeply Virtual Compton Scattering and its t-Dependence at HERA**, F.D. Aaron et al. [H1-Coll.], DESY 07 – 142, arXiv:0709.4114 [hep-ex], Phys.Lett. **B659** (2008), 796.

[9] **Measurement of Isolated Photon Production in Deep-Inelastic Scattering at HERA**, F.D. Aaron et al. [H1-Coll.], DESY 07 – 147, arXiv:0711.4578 [hep-ex], Eur.Phys.J. **C54** (2008), 371.

[10] **Three- and Fourjet Production in Deep Inelastic ep Scattering and Low x Parton Dynamics at HERA**, F.D. Aaron et al. [H1-Coll.], DESY 07 – 200, arXiv:0711.2606 [hep-ex], Eur.Phys.J. **C54** (2008), 389.

[11] **Search for Excited Neutrinos at HERA**, F.D. Aaron et al. [H1-Coll.], DESY 08 – 009, arXiv:0802.1858 [hep-ex], Phys.Lett. **B** (2008), in print.

[12] Contributed papers by the H1-Coll. to EPS2007 (HEP2007), Int. Europhysics Conf. on High Energy Physics, Manchester, UK, 19-25 July 2007; only those papers are listed, which have not yet been submitted to journals or to previous conferences.

[13] **D^* Production in Deep Inelastic Scattering with the H1 Detector** [12]

[14] **Inelastic Electroproduction of J/Ψ Mesons at HERA** [12]

[15] **Beam Charge Azimuthal Asymmetry in Deeply Virtual Compton Scattering at HERA II** [12]

[16] **Inclusive ep Scattering Cross Section at High Q^2 and High y** [12]

[17] **Measurement of the Inclusive ep Scattering Cross Section at Low Q^2 and x at HERA** [12]

[18] **Inclusive ep Scattering Cross Section at Low Q^2**

and High y [12]

[19] **Inclusive Jet Production in Deep Inelastic Scattering at Low and Medium Q^2 at HERA** [12]

[20] **Minijet Production in Deep Inelastic Scattering at HERA** [12]

[21] **Inclusive Jet Production at High Q^2 (HERA II)** [12]

[22] **Precision Measurements of α_s at HERA using Jets at High Q^2 (H1+ZEUS)** [12]

[23] **A Combined H1 and ZEUS Measurement of Events with Isolated Leptons and Missing P_t at HERA** [12]

[24] **Multi-Lepton Events at HERA** [12]

[25] **Events with an Isolated Lepton (Electron or Muon) and Missing Transverse Momentum at HERA** [12]

[26] **Combined Electroweak and QCD Fit of Inclusive NC and CC Data with Polarised Lepton Beams at HERA** [12]

[27] **Measurement of W Production and W Polarisations at HERA** [12]

[28] **A General Search for New Phenomena at HERA** [12]

[29] **A Search for Excited Electrons in ep Collisions at HERA** [12]

[30] **Events with an Isolated Tau Lepton and Missing Transverse Momentum at HERA** [12]

[31] **Search for Single Top Production at HERA** [12]

[32] **Isolated Photon Production in Deep Inelastic Scattering at HERA**, Carsten Schmitz, PhD Thesis, University of Zürich (2007) available at *http://www-h1.desy.de/publications/theses_list.html*.

[33] Physik-Institut, University of Zürich, Annual Reports 1996/7 ff.; available at *http://www.physik.unizh.ch/reports.html*.

[34] **A Vertex Trigger based on Cylindrical Multiwire Proportional Chambers**,
J. Becker, K. Bösiger, L. Lindfeld, K. Müller, P. Robmann, S. Schmitt, C. Schmitz, S. Steiner, U. Straumann, K. Szeker, P. Truöl, M. Urban, A. Vollhardt, N. Werner, D. Baumeister, S. Löchner, and M. Hildebrandt, physics/0701002, Nucl.Instr.Meth. **A586** (2008), 190.

[35] Preliminary results presented by members of the H1-collaboration at the 2008 Workshop on Deep Inelastic Scattering (DIS 2008), London, April 7-11, 2008; available at *http://www-h1.desy.de/publications/H1preliminary.short_list.html*

[36] A. Gehrmann-De Ridder, T. Gehrmann, and E. Poulsen, Phys.Rev.Lett. **96** (2006), 132002; Eur.Phys.J.**C47** (2006), 395.

[37] A. Gehrmann-De Ridder, G. Kramer and H. Spiesberger, Nucl.Phys. **B578** (2000) 326.

[38] A. Gehrmann-De Ridder, T. Gehrmann and E. Poulsen, Eur.Phys.J. **C47** (2006) 395 [hep-ph/0604030].

[39] D. Buskulic *et al.* [ALEPH Coll.], Zeitschrift für Physik **C69** (1996) 365.

[40] A. Aktas *et al.* [H1-Coll.], Eur.Phys.J. **C38** (2005) 437.

[41] M. Fontannaz, J. P. Guillet and G. Heinrich, Eur.Phys.J. **C21** (2001) 303.

[42] A. V. Lipatov and N. P. Zotov, Phys.Rev. **D72** (2005) 054002.